Synergistic enhancement of CdSe/ZnS quantum dot and liquid scintillator for radioluminescent nuclear batteries

Zhiheng Xu[1,2,#], Zhengrong Zhang[1,#], Kelum A. A. Gamage[3,] Yunpeng Liu[1,2], Huangfeng Ye[1], Xiaobin Tang[1,2,*]

[1]Department of Nuclear Science and Technology, Nanjing University of Aeronautics and Astronautics, Nanjing 210016, China

[2]Key Laboratory of Nuclear Technology Application and Radiation Protection in Astronautics (Nanjing University of Aeronautics and Astronautics), Ministry of Industry and Information Technology, Nanjing 210016, China

[3]Electronics & Electrical Engineering, James Watt School of Engineering, University of Glasgow, Glasgow, G12 8QQ, United Kingdom

*Corresponding E-mail: tangxiaobin@nuaa.edu.cn

# Zhiheng Xu and Zhengrong Zhang contributed equally to this work.

Summary

The feasibility of utilizing CdSe/ZnS quantum dots (QDs) in liquid scintillator radioluminescent nuclear batteries to improve battery performance was studied. The peak position of the radioluminescence emission spectra of liquid scintillator can be regulated by controlling the QD components. This method is suitable for obtaining a satisfactory spectral matching between fluorescence materials and photovoltaic devices to increase the output performance of the battery. In the experiment, CdSe/ZnS QDs were introduced into Emulsifier-Safe liquid scintillator, and the output properties of radioluminescent nuclear batteries were investigated via X-ray. Results indicate that the battery with 15 mg CdSe/ZnS QDs generated the best electric power under different tube voltages. To analyze the X-ray radioluminescence effects of the liquid scintillator, the radioluminescence spectra of the Emulsifier-Safe with and without CdSe/ZnS QDs were measured and compared. The spectral matching degree between the Emulsifier-Safe with different concentrations of CdSe/ZnS QDs and the GaAs device was also analyzed by considering luminescence utilization in batteries. This framework can serve as a guide for the development of radioluminescent material system for long-lasting, high-performance power supplies.

KEYWORDS: quantum dot, liquid scintillator, nuclear battery, energy conversion

1. INTRODUCTION

Nuclear batteries have great application prospects in space exploration, seabed monitoring and portable electronic equipment due to their advantages of high energy density, long life, strong environmental adaptability, and wide selection of materials.[1,2] As a representative of particle-transduced nuclear batteries, radioluminescent nuclear battery is proposed and developed on the basis of a mature and thorough study of radiovoltaic nuclear battery techniques.[3–5] The main difference between the radioluminescent and radiovoltaic nuclear batteries lies in the former adds an intermediate energy conversion process, whereas the integrated battery structure adds a fluorescence material.[6–8] The entire energy conversion process of radioluminescent nuclear battery is from nuclear energy to light energy, which is then reconverted into electrical energy, which mainly includes the radioluminescence (RL) effect and photovoltaic (PV) effect.[9] The scintillator material can convert high-energy radiation particles into low-energy visible light, and then combined with energy conversion technology can achieve electrical energy supply and reduce the radiation damage effect of PV devices.[10,11] Different types of radiation particles can be considered as the excitation sources of nuclear batteries, among which X-ray has strong penetrating ability and weak radiation damage effect on devices.[12–15] X-ray-based long-life self-powered technology has broad application prospects in many fields such as radiation safety testing, communication sensing, and high-energy physics research, especially for the special needs of deep space exploration.[16,17]

As one kind of mature fluorescence materials, liquid scintillators are directly sensitive to X-rays or gamma radiation and can be used to change the spectral wavelength of the rays to the region of visible light.[18,19] Furthermore, liquid scintillators are organic scintillators with high luminous efficiency and are characterized by their low price, adequate attenuation length, long stability (with careful chemical treatment), good plasticity, and inherent radiation resistance.[20,21] Liquid scintillation can effectively absorb X-rays, enhance the efficiency of ray capture, and improve the RL response through inelastic scattering. Given these characteristics, liquid scintillators are promising candidates for intermediate energy conversion materials in X-ray nuclear batteries. However, the matching between the liquid scintillators and the photovoltaic device is not highly satisfactory. As a new type of luminescent materials, quantum dots (QDs) have the characteristics of high fluorescence quantum efficiency, high carrier

mobility, adjustable emission wavelength, and good emission stability.[22–24] The Stokes shift of QDs can effectively regulate the emission wavelength of RL. Therefore, QDs were introduced into liquid scintillator to regulate the emission spectrum and match the peak of the external quantum efficiency (EQE) curve of the photovoltaic device.[25–27] This process provides a feasible candidate for effectively improving battery performance.[28,29] And as of now, nuclear batteries based on liquid scintillators doped with QDs have been rarely reported. The characteristics of X-ray radioluminescent nuclear batteries based on Emulsifier-Safe liquid scintillator with and without CdSe/ZnS QDs under various X-ray intensities were investigated.

The battery structure proposed by this research is shown in Fig. 1, which includes three parts: X-ray emitter, liquid scintillator doped with QDs, and GaAs device. The liquid scintillator absorbs X-ray energy and produces RL (about 420 nm blue-violet light). CdSe/ZnS QDs in liquid scintillator can convert the blue-violet light to the longer wavelength luminescence, which can effectively generate electron-hole pairs in the GaAs photovoltaic device, and separate and aggregate to the two ends under the action of the built-in electric field to form a potential difference. Finally, the battery delivers an output current after being connected to an external circuit. In this work, we explored the effects of CdSe/ZnS QDs and liquid scintillators on the modulation and enhancement of fluorescence, and performed performance analysis based on radioluminescent nuclear batteries.

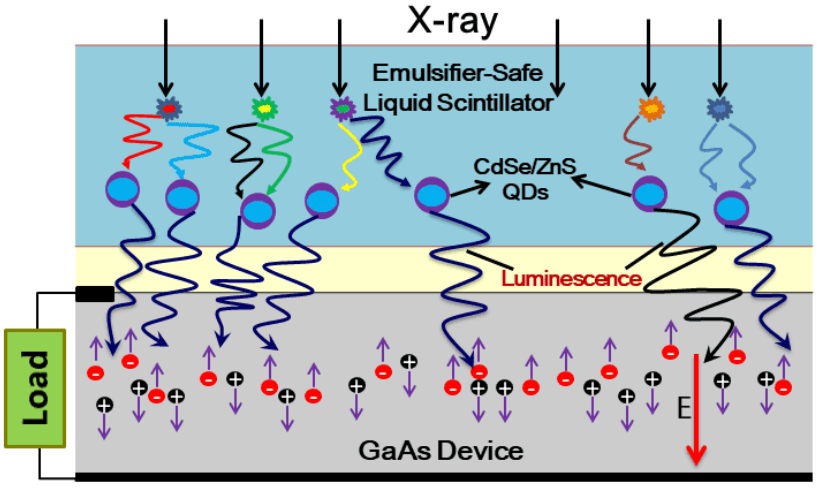

Fig. 1. Schematic of radioluminescent nuclear battery based on X-ray, GaAs device and Emulsifier-Safe liquid scintillator doped with CdSe/ZnS QDs.

2. MATERIALS AND METHODS

Emulsifier-Safe liquid scintillator (PerkinElmer 6013381, USA) was used as

fluorescence material for battery due to its high flash points, good stability, and low toxicity. Fluorescence lifetime τ and quantum yield φ_f were measured by a steady-state and transient-state fluorescence spectrometer (Edinburgh Instruments FLS980, the UK).τ represents the average time when particles exist in an excited state, which is related to the type of scintillator, activator of the scintillator, concentration of the wavelength shifter, and temperature. φ_f can be calculated using the following formula:

$$\varphi_f = \frac{K_f}{K_f + \sum K_i} \tag{1}$$

where K_f is the rate constant of fluorescence emission, and ΣK_i is the sum of the rate constants for non-radiative transitions such as intersystem crossings. Under the ultraviolet light excitation of 400 nm, Emulsifier-Safe possessed fluorescence lifetime τ of 1.7 ns and fluorescence quantum yield φ_f of 96.5%.

Based on the hot injection method, CdSe/ZnS QDs were prepared by reacting cadmium oxide (CdO), selenium (Se), zinc acetate dihydrate ($C_4H_{10}O_6Zn$), and sodium sulphide ($Na_2S{\cdot}9H_2O$) in octadecylene solution. The optical properties of the fluorescent material were obtained by a Cary Eclipse fluorescence spectrophotometer (Agilent Technologies G9800a, Malaysia) and a UV/Vis spectrophotometer (Shimadzu UV-2550, Japan). As shown in Fig. 2, the excitation and emission peak wavelength of Emulsifier-Safe are approximately 396 and 420 nm, and the emission peak wavelength of CdSe/ZnS QDs is approximately 520 nm.

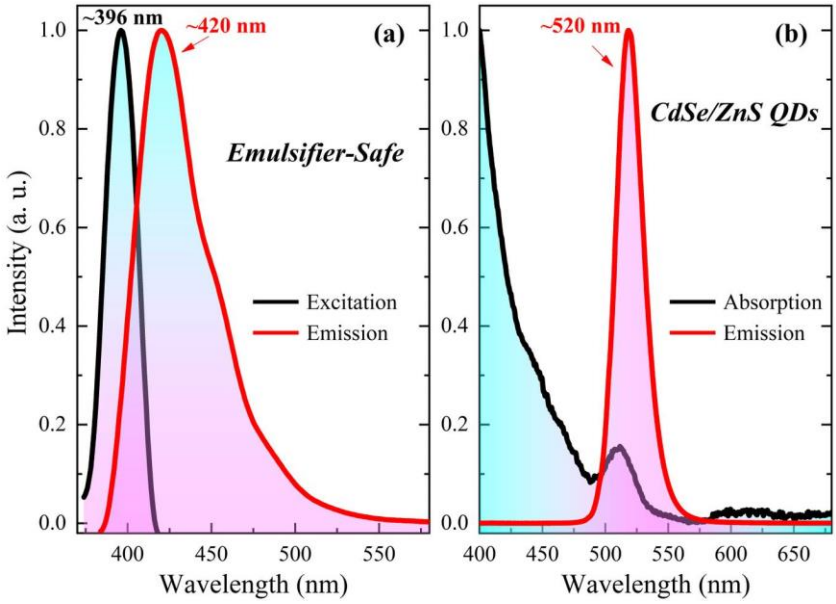

Fig. 2. Optical spectra of (a) Emulsifier-Safe and (b) CdSe/ZnS QDs.

The excitation source used for the measurement of the RL emission spectra of

these fluorescent materials is X-rays. A 50 W Mo X-ray tube (Shanghai KeyWay Electron Company Ltd. KYW900A, China) was used as a suitable substitute for the low-energy X-ray source due to safety concerns and convenience. The X-ray tube was operated with tube voltage U of 30 to 50 kV and tube current I of 800 μA. The tube voltage was adjusted so that the accelerated electrons can obtain the X-ray with different average energy levels. The basic specifications of the X-ray tube are listed in Table S1. X-ray energy spectra were obtained by a silicon drift detector (AMPTEK X-123, USA) under the excitation condition of 30 to 50 kV tube voltage (Fig. 3).

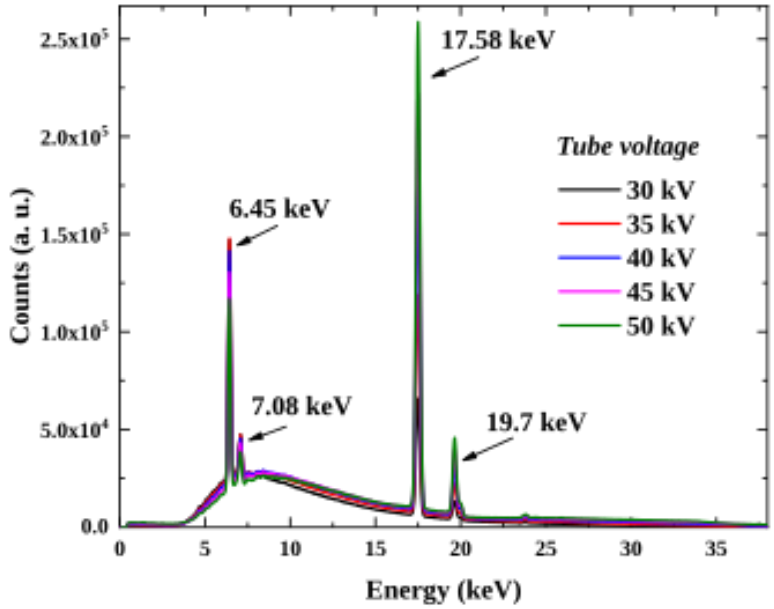

Fig. 3. X-ray energy spectra for a tube voltage of 30–50 kV.

3. RESULTS AND DISCUSSION

3.1 Optical properties of liquid luminescent materials

Different amounts (0–20 mg) of CdSe/ZnS QDs powder were added to the same volume (8 mL) of Emulsifier-Safe liquid scintillation solution to discuss their RL properties. The mixture was then placed in an ultrasonic disperser for about 5 minutes in order to distribute evenly QDs powder. Under the chosen X-ray tube (tube voltage: 30, 35, 40, 45, and 50 kV; tube current: 800 μA) excitation, the patterns of the RL emission spectra of the Emulsifier-Safe doped with 0, 1, 2, 3, 4, 5, 10, 15, and 20 mg of CdSe/ZnS QDs are also constantly changing, as shown in Fig. 4. Before the addition of CdSe/ZnS QDs, the emission peak wavelength of the pure Emulsifier-Safe has only one main peak at about 420 nm. With the gradual addition of QDs, a new and stronger main peak appeared at approximately 520 nm in the mixture. As more and more QDs were dissolved in Emulsifier-Safe liquid scintillator, the colour of the mixture turned from

blue to blue-green then to a deep, steady yellow-green. The spectral curve also shows a changing trend one after another. The relative luminescence intensities at 520 nm increased significantly with the increasing amount of CdSe/ZnS QDs. Conversely, the RL relative intensities at 420 nm decreased with the increasing QDs. As the amount of CdSe/ZnS QDs in the mixed liquid increases, the QDs can absorb more RL from the liquid scintillator. The photoluminescence relative intensities at 520 nm reached the maximum when 20 mg of CdSe/ZnS QDs were completely dissolved in 8 mL of Emulsifier-Safe liquid scintillator. The added QDs serve a dual function, which can not only effectively transfer the RL peak wavelength of the liquid scintillation, and also efficiently absorb fluorescent photons and improve the overall luminescence emission intensity.[30–32] Moreover, the relative RL intensity of the Emulsifier-Safe was enhanced with increasing tube voltage, but the peak wavelengths remained steady and unchanged.

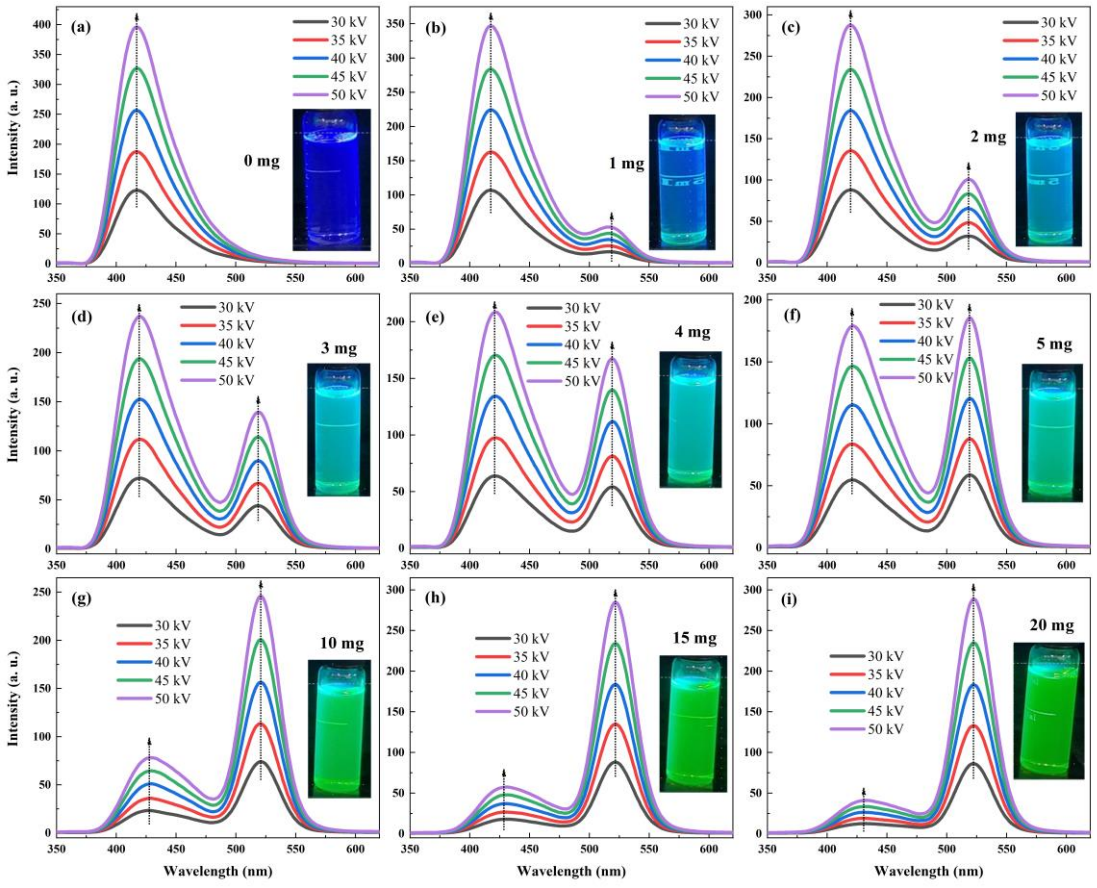

Fig. 4. RL emission spectra of Emulsifier-Safe doped with (a) 0, (b) 1, (c) 2, (d) 3, (e) 4, (f) 5, (g) 10, (h) 15, and (i) 20 mg CdSe/ZnS QDs. Illustrations are the pictures of these experimental samples illuminated by 365 nm ultraviolet light.

It is worth noting that in this process, the amount of QDs should also be controlled. Comparing before and after adding a certain amount of QDs, the peak emission

wavelength of these mixed samples has effectively shifted, but the overall relative RL intensity has also decreased to a certain extent. Although the more the amount of QDs, the stronger the light absorption, but it will also reduce the transmission of the fluorescent material (Fig. 5). The absorbance (A) and transmittance (T) can be expressed as follows:

$$A = \lg(1/T) = \lg(I_0 / I_t) \quad (2)$$

where I_0 is the intensity of incident light, and I_t is the intensity of transmission light. The transmittance of the mixed liquor decreases with the increase of QDs amount. A series of troughs at 490–530 nm was observed in the transmittance curves after the addition of CdSe/ZnS QDs in the liquid scintillator. The transmittance decreased by about 25% at around 515 nm, when the QDs amount increased from 10 mg to 20 mg. As the content of QDs in the mixed liquid increases, the RL intensity at the peak emission wavelength of the liquid scintillation at 420 nm gradually decreases, and at the same time, the turbidity of the solution also increases, the self-absorption effect is stronger, and the intensity at the peak wavelength of 520 nm also decreases. Therefore, the luminescence intensity of the mixed liquid was weakened by the high density of CdSe/ZnS QDs in the liquid scintillator.

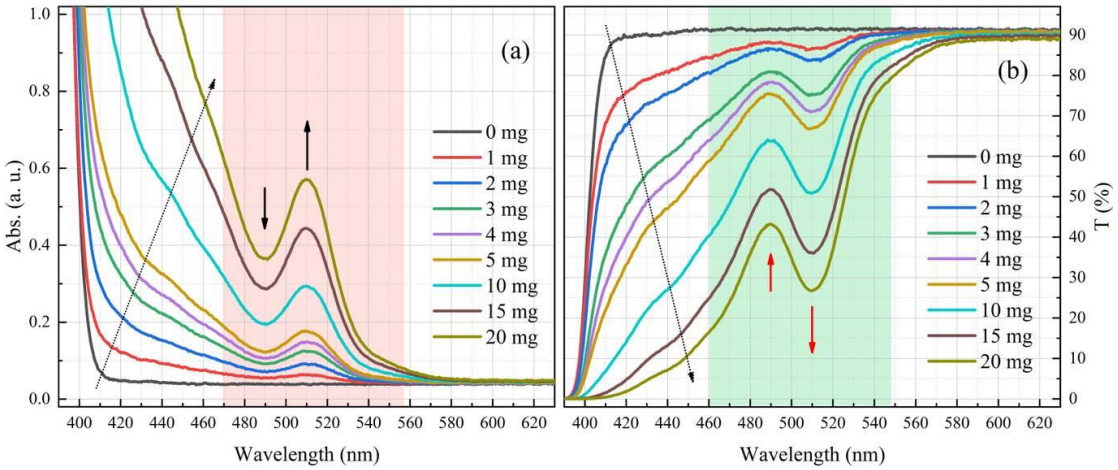

Fig. 5. (a) Absorption and (b) transmission spectra of the Emulsifier-Safe liquid scintillator doped with different amounts (0, 1, 2, 3, 4, 5, 10, 15, and 20 mg) of CdSe/ZnS QDs.

Fig. 6 reflects the RL test result pictures of Emulsifier-Safe doped with 0, 15, and 20 mg of CdSe/ZnS QDs. The closer to the X-ray emission port, the stronger the intensity of the RL. As the tube voltage increases, the X-ray field and range also gradually expand. Moreover, the luminescence intensities increased significantly with

increasing tube voltage and reached the maximum at tube voltages as high as 50 kV, as well as the other cases (Emulsifier-Safe doped with 1, 2, 3, 4, 5, and 10 mg of CdSe/ZnS QDs). Fig. 7 shows the photon count statistics of Emulsifier-Safe on the horizontal plane under the excitation condition of 50 kV tube voltage, based on the results of multiple measurements by the camera.

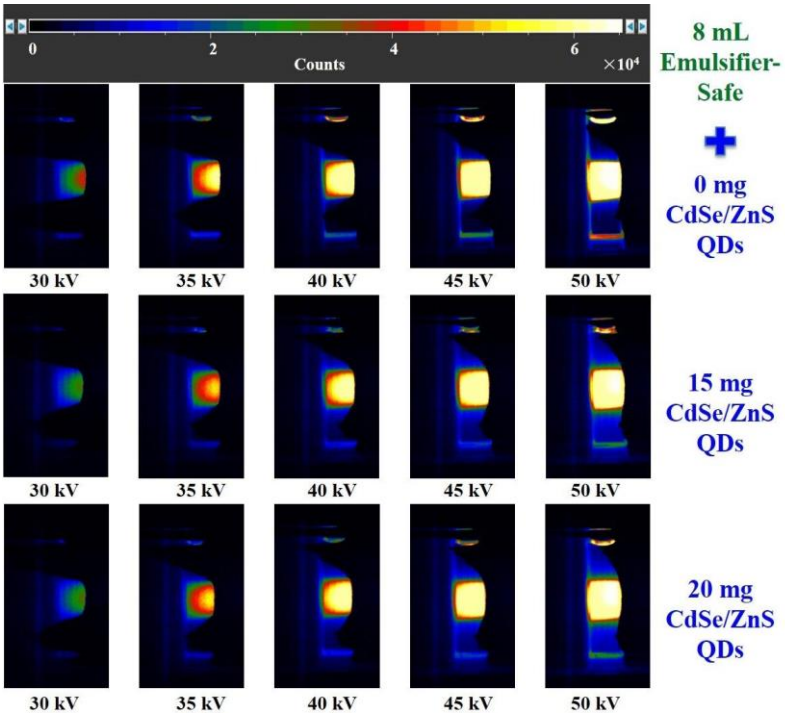

Fig. 6. Images of Emulsifier-Safe doped with 0, 15, and 20 mg CdSe/ZnS QDs under different X-ray parameters (tube voltage: 30, 35, 40, 45, and 50 kV; tube current: 800 μA) excitation were taken by EMCCD camera.

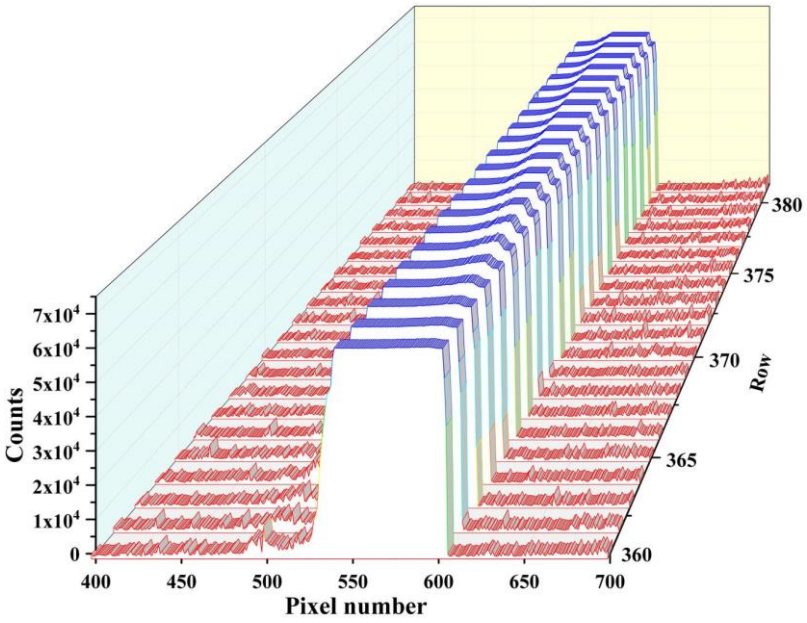

Fig. 7. Counting statistics of RL images of Emulsifier-Safe taken by EMCCD camera under 50 kV tube voltage.

3.2 Spectral coupling and matching analysis

GaAs device was used as the photoelectric converter of radioluminescent nuclear battery due to direct bandgap, large light absorption coefficient, wide bandgap, low leakage currents, high radiation resistance and a series of advantages.[33–35] The spectral response of the GaAs device to the fluorescent material is shown in Fig. 8. But before adding CdSe/ZnS QDs, when there is only Emulsifier-Safe, the emitted RL was mainly concentrated in the low response section. As the amount of QDs increases, the peak wavelength was red-shifted, and the luminous intensity gradually increased, as well as the proportion in the high response interval of the GaAs device. The higher the amount of QDs in the liquid scintillation system, the more the peak wavelength of the RL emission shifts from 420 nm to 520 nm, which is also more conducive to the absorption application of GaAs device (normalized EQE can be as high as 90%~97.5%). Even though the overall RL intensity was lost to some extent after mixing the Emulsifier-Safe and CdSe/ZnS QDs, the photoelectric response capacity of the adjusted RL emission spectra under the GaAs devices were greatly improved.

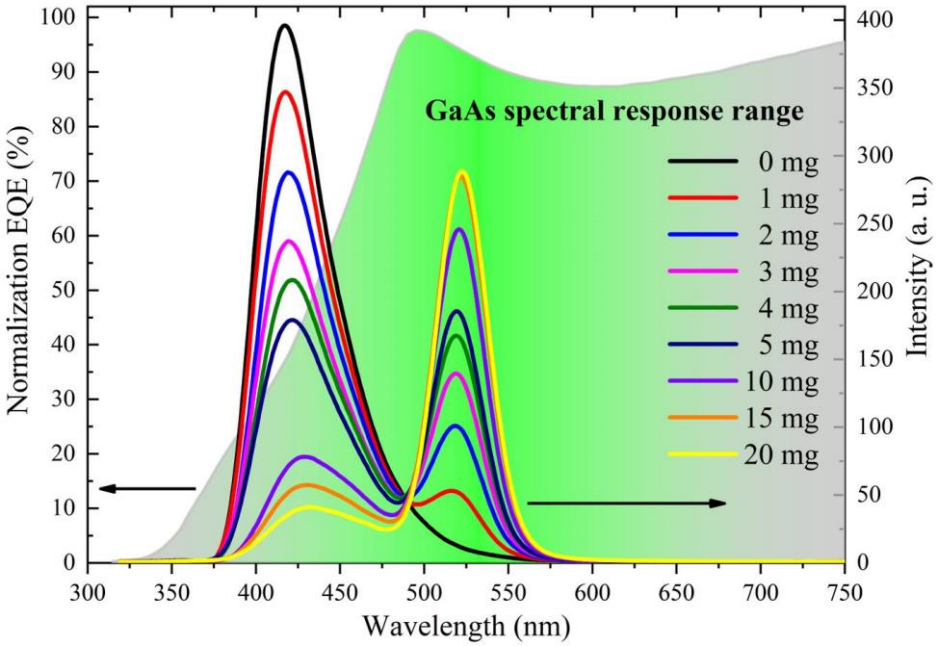

Fig. 8. Normalized EQE of the GaAs device and RL emission spectra of Emulsifier-Safe doped with CdSe/ZnS QDs under excitation of 50 kV tube voltage and 800 μA tube current.

3.3 Electrical performance of liquid nuclear battery

The *I–V* characteristic curves of radioluminescent nuclear batteries were measured by a dual-channel system source-meter instrument (Keithley Model 2636A, USA) at room temperature. Fig. 9 shows the changes in electrical properties of the batteries at different tube voltages as a function of CdSe/ZnS QDs amount (0–20 mg).

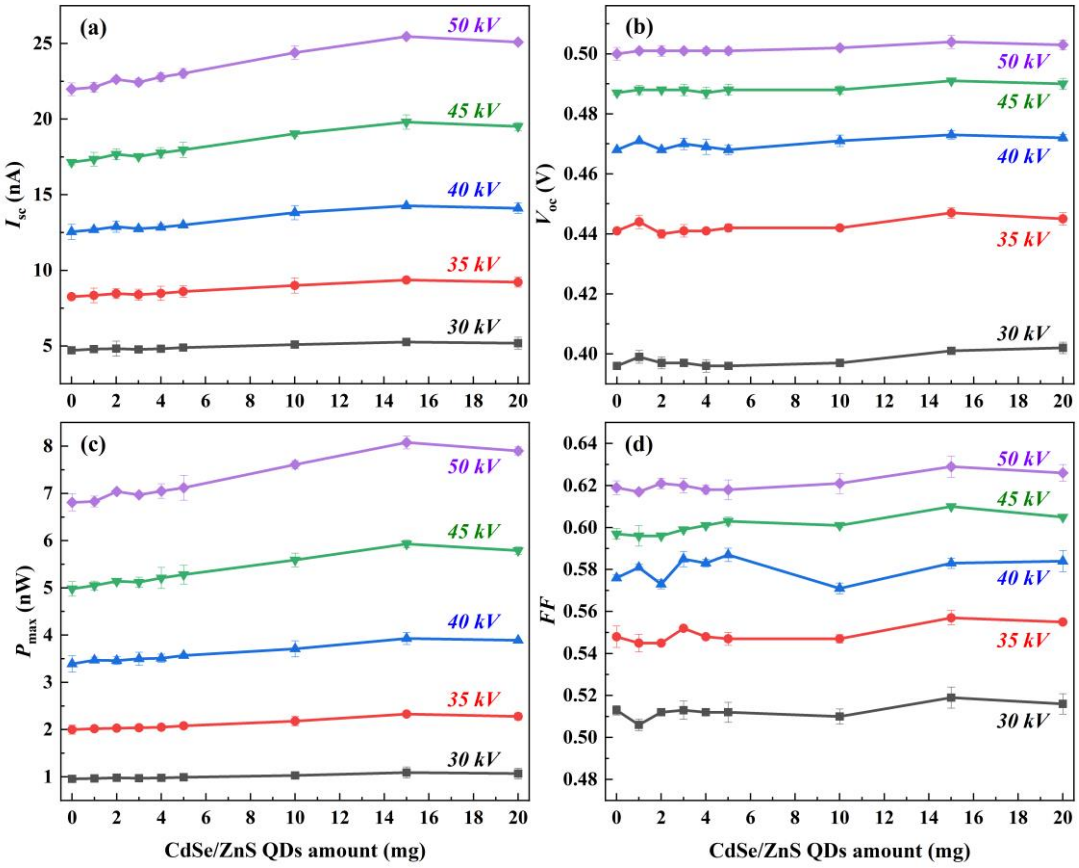

Fig. 9. Electrical properties of the batteries at different tube voltages as a function of CdSe/ZnS QDs amount: (a) I_{sc}, (b) V_{oc}, (c) P_{max}, and (d) *FF*. The tube current remained unchanged at 800 μA.

Under the excitation of a specific tube voltage, with the increase of the QDs amount, the short-circuit current (I_{sc}) and maximum output power (P_{max}) gradually increased and reached saturation, but although the values of the open-circuit voltage (V_{oc}) and fill factor (*FF*) fluctuate, the overall change was not large. As the tube voltage increases, the performance optimization effect is more obvious. However, there are also competitions and trade-offs in this process. After adding about 15 mg of CdSe/ZnS QDs, the effect of spectrum adjustment can make the battery output power reach a better value. The output performance of the battery with 20 mg of QDs is lower than that with 15 mg. This is mainly because the amount of QDs continues to increase, the light transmittance of the mixed liquid gradually decreases, but the increase in light intensity

value is not large enough. Moreover, the luminescence intensity at 520 nm is almost similar for 15 and 20 mg of QDs, but the luminescence intensity for 20 mg of QDs is less than that for 15 mg at 420 nm. From the above optical and electrical performance test results, it can be seen that under the experimental conditions when the amount of quantum dots added is about 15 mg, it is relatively advantageous in a comprehensive contest of all parties. Therefore, it can be known that optimizing the coupling response between energy conversion components in the radioluminescent nuclear battery can effectively improve its overall output performance.

4. CONCLUSIONS

The liquid scintillator radioluminescent nuclear battery enhanced by CdSe/ZnS QDs was demonstrated by using an X-ray tube to be equivalent to a series of low-energy X-ray sources. The RL intensity at 520 nm increased significantly with increasing CdSe/ZnS QDs in Emulsifier-Safe under the same excitation condition. As the proportion of QDs in the mixed solution increases, the corresponding transmittance gradually decreases, and the degree of spectral coupling response between the fluorescent material and GaAs device is also enhanced. As a consequence, when 15 mg CdSe/ZnS QDs are added, the P_{max} of the battery is increased by 19.19% compared with the Emulsifier-Safe liquid scintillator only, under the excitation of X-ray at 45 kV tube voltage and 800 μA tube current. On the basis of liquid scintillation, QD doping is used to control the emission wavelength, thereby improving the coupling and matching of the spectrum, improving energy utilization, and optimizing the performance of the nuclear battery. The synergistic enhancement effect and energy conversion technology can also be effectively applied to more fields of optical detection and sensing.

SUPPLEMENTARY MATERIAL

See supplementary material for more information about the optical properties of Emulsifier-Safe liquid scintillator, the microscopic characterization of CdSe/ZnS QDs, and experimental materials and test devices.

CONFLICT OF INTEREST

None.

ORCID

Zhiheng Xu https://orcid.org/0000-0002-9229-8558

Xiaobin Tang https://orcid.org/0000-0003-3308-0468

ACKNOWLEDGEMENTS

This research was supported by the National Natural Science Foundation of China (Grant Nos. 11675076 and 12005101); the Project supported by China Postdoctoral Science Foundation (Grant No. 2019M661836); the Fundamental Research Funds for the Central Universities (Grant No. NP2018462).

REFERENCES

1. Prelas MA, Weaver CL, Watermann ML, Lukosi ED, Schott RJ, Wisniewski DA. A review of nuclear batteries. *Prog. Nucl. Energ.* 2014;75:117-148.
2. Russo J, Litz MS, William Ray II, Berk H, Cho H, Bigio DI, Weltz A, Alam TR. Planar and textured surface optimization for a tritium-based betavoltaic nuclear battery. *Int. J. Energ. Res.* 2019;43(9):4370-4389.
3. Sharma A, Melancon JM, Bailey SG, Zivanovic SR. Betavoltaic cells using P3HT semiconductive conjugated polymer. *IEEE T. Electron Dev.* 2015;62:2320-2326.
4. Borisyuk PV, Yakovlev VP, Vasiliev OS, Lebedinskii YY, Fetisov VV, Kozlova TI, Kozodaev MG. Size-ordered ^{63}Ni nanocluster film as a betavoltaic battery unit. *Appl. Phys. Lett.* 2018;112:143105.
5. Xu ZH, Liu YP, Zhang ZR, Chen W, Yuan ZC, Liu K, Tang XB. Enhanced radioluminescent nuclear battery by optimizing structural design of the phosphor layer. *Int. J. Energ. Res.* 2018;42(4):1729-1737.
6. Bower KE, Barbanel YA, Shreter YG, Bohnert GW. Polymers, phosphors, and voltaics for radioisotope microbatteries, CRC press, Boca Raton, FL, USA. 2002.
7. Lu M, Zhang GG, Fu K, Yu GH, Su D, Hu JF. Gallium nitride schottky betavoltaic nuclear batteries. *Energ. Convers. Manage.* 2011;52(4):1955-1958.
8. Liu YP, Tang XB, Xu ZH, Hong L, Wang P, Chen D. Optimization and temperature effects on sandwich betavoltaic microbattery. *Sci. China Technol. Sc.* 2014;57(1):14-18.
9. Xu ZH, Liu YP, Zhang ZR, Chen W, Yuan ZC, Liu K, Tang XB. Enhanced radioluminescent nuclear battery by optimizing structural design of the phosphor layer. *Int. J. Energ. Res.* 2018;42(4):1729-1737.

10. Zhang ZR, Liu YP, Tang XB, Xu ZH, Yuan ZC, Liu K, Chen W. GaAs low-energy X-ray radioluminescence nuclear battery. *Nucl. Instrum. Methods Phys. Res. B.* 2018;415:9-16.
11. Yu DJ, Wang P, Cao F, Gu Y, Liu JX, Han ZY, Huang B, Zou YS, Xu XB, Zeng HB. Two-dimensional halide perovskite as β-ray scintillator for nuclear radiation monitoring. *Nat. Commun.* 2020;11(1):1-10.
12. Artun O. A study of nuclear structure for ^{244}Cm, ^{241}Am, ^{238}Pu, ^{210}Po, ^{147}Pm, ^{137}Cs, ^{90}Sr and ^{63}Ni nuclei used in nuclear battery. *Mod. Phys. Lett. A.* 2017;32(22):1750117.
13. Butera S, Whitaker M DC, Lioliou G, Barnett AM. AlGaAs ^{55}Fe X-ray radioisotope microbattery. *Sci. Rep.* 2016;6(1):38409.
14. Butera S, Lioliou G, Krysa AB, Barnett AM. $Al_{0.52}In_{0.48}P$ ^{55}Fe X-ray-photovoltaic battery. *J. Phys. D Appl. Phys.* 2016;49(35):355601.
15. Lioliou G, Meng X, Ng JS, Barnett AM. Temperature dependent characterization of gallium arsenide X-ray mesa pin photodiodes. *J. Appl. Phys.* 2016;119(12):124507.
16. Wei HT, Fang YJ, Mulligan P, Chuirazzi W, Fang HH, Wang CC, Ecker BR, Gao YL, Loi MA, Cao L, Huang JS. Sensitive X-ray detectors made of methylammonium lead tribromide perovskite single crystals. *Nat. Photonics.* 2016;10(5):333-339.
17. Walton R, Anthony C, Ward M, Metje N, Chapman DN. Radioisotopic battery and capacitor system for powering wireless sensor networks. *Sensor. Actuat. A-Phys.* 2013;203:405-412.
18. Xu ZH, Jin ZG, Tang XB, Liu YP, Guo X, Peng C, Wang HY. Designing performance enhanced nuclear battery based on the Cd-109 radioactive source. *Int. J. Energ. Res.* 2020;44(1):508-517.
19. Chen QS, Wu J, Ou XY, Huang BL, Almutlaq J, Zhumekenov AA, Guan XW, Han SY, Liang LL, Yi ZG, Li J, Xie XJ, Wang Y, Li Y, Fan DY, Teh D BL, All AH, Mohammed OF, Bakr OM, Wu T, Bettinelli M, Yang HH, Huang W, Liu XG. All-inorganic perovskite nanocrystal scintillators. *Nature.* 2018;561(7721):88-93.
20. Swiderski L, Moszyński M, Wolski D, Iwanowska J, Szczśniak T, Schotanus P, Hurlbut C. Suppression of gamma-ray sensitivity of liquid scintillators for neutron detection. *Nucl. Instrum. Methods Phys. Res. A.* 2011;652(1):330-333.

21. Chang Z, Okoye NC, Urffer MJ, Green AD, Childs KE, Miller LF. On the scintillation efficiency of carborane-loaded liquid scintillators for thermal neutron detection. *Nucl. Instrum. Methods Phys. Res. A.* 2015;769:112-122.
22. Pevere F, Treskow CV, Marino E, Anwar M, Bruhn B, Sychugov I, Linnros J. X-ray radiation hardness and influence on blinking in Si and CdSe quantum dots. *Appl. Phys. Lett.* 2018;113(25):253103.
23. Yang DD, Li XM, Zhou WH, Zhang SL, Meng CF, Wu Y, Wang Y, Zeng HB. $CsPbBr_3$ quantum dots 2.0: benzenesulfonic acid equivalent ligand awakens complete purification. *Adv. Mater.* 2019;31(30):1900767.
24. Ye S, Guo JQ, Song J, Qu JL. Achieving high-resolution of 21 nm for STED nanoscopy assisted by CdSe@ZnS quantum dots. *Appl. Phys. Lett.* 2020;116(4):041101.
25. Litvin AP, Martynenko IV, Purcell-Milton F, Baranov AV, Fedorov AV, Gun'ko YK. Colloidal quantum dots for optoelectronics. *J. Mater. Chem. A.* 2017;5(26):13252-13275.
26. Li XM, Cao F, Yu DJ, Chen J, Sun ZG, Shen YL, Zhu Y, Wang L, Wei Y, Wu Y, Zeng HB. All inorganic halide perovskites nanosystem: synthesis, structural features, optical properties and optoelectronic applications. *Small.* 2017;13(9):1603996.
27. Du ZL, Artemyev M, Wang J, Tang JG. Performance improvement strategies for quantum dot-sensitized solar cells: a review. *J. Mater. Chem. A.* 2019;7(6):2464-2489.
28. Zhang ZR, Tang XB, Liu YP, Zhou DY, Xu ZH, Wu M, Cao ZY. Use the indirect energy conversion of the phosphor layer to improve the performance of nuclear batteries. *Energy Technol.* 2018;6:1959-1965.
29. Xu ZH, Tang XB, Liu YP, Zhang ZR, Chen W, Yuan ZC, Liu K. ZnS:Cu phosphor layers as energy conversion materials for nuclear batteries: a combined theoretical and experimental study of their geometric structure. *Energy Technol.* 2017;5(9):1638-1646.
30. Yang DD, Li XM, Wu Y, Wei CT, Qin ZY, Zhang CF, Sun ZG, Li YL, Wang Y, Zeng HB. Surface halogen compensation for robust performance enhancements of $CsPbX_3$ perovskite quantum dots. *Adv. Opt. Mater.* 2019;7(11):1900276.
31. Chen W, Tang XB, Liu YP, Xu ZH, Yuan ZC, Zhang ZR, Liu K. Radioluminescent

nuclear battery containing $CsPbBr_3$ quantum dots: Application of a novel wave-shifting agent. *Int. J. Energ. Res.* 2019;43(9):4520-4533.

32. Xu ZH, Tang XB, Liu YP, Zhang ZR, Chen W, Liu K, Yuan ZC. $CsPbBr_3$ quantum dot films with high luminescence efficiency and irradiation stability for radioluminescent nuclear battery application. *ACS Appl. Mater. Interfaces* 2019;11(15):14191-14199.
33. Chen H, Jiang L, Chen XY. Design optimization of GaAs betavoltaic batteries. *J. Phys. D Appl. Phys.* 2011;44(21):215303.
34. Butera S, Lioliou G, Barnett AM. Gallium arsenide ^{55}Fe X-ray-photovoltaic battery. *J. Appl. Phys.* 2016;119:064504.
35. Spencer MG, Alam T. High power direct energy conversion by nuclear batteries. *Appl. Phys. Rev.* 2019;6(3):031305.

Graphical Table of Contents

Synergistic enhancement of CdSe/ZnS quantum dot and liquid scintillator for radioluminescent nuclear batteries

*Zhiheng Xu, Zhengrong Zhang, Kelum A. A. Gamage, Yunpeng Liu, Huangfeng Ye, Xiaobin Tang**

***Corresponding author:**

Xiaobin Tang, Department of Nuclear Science and Technology, Nanjing University of Aeronautics and Astronautics, Nanjing 210016, China.

E-mail: tangxiaobin@nuaa.edu.cn

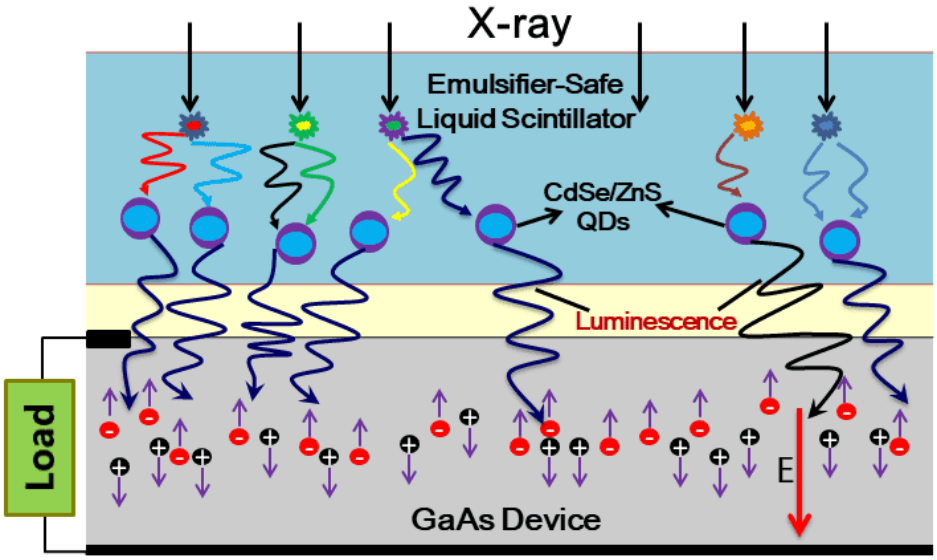

Brief Description/Graphical abstract: A technique that uses liquid scintillator and quantum dots coordinated regulation technology to optimize the performance of radioluminescent nuclear battery is proposed. Liquid scintillation converts radiant energy into light energy, and quantum dots adjust emission wavelength on this basis. This synergistic regulation and enhancement effect of nanomaterials can effectively improve the output performance of optoelectronic devices. Such nanomaterials provide a new idea for the development of energy conversion technologies and open up endless possibilities for their application.